ELSEVIER
Journal of Applied Geophysics 34 (1996) 291–305
APPLIED GEOPHYSICS

Transient response of a homogeneous half space with due regard for displacement currents

M. Goldman [a], V. Mogilatov [b], M. Rabinovich [c]

[a] Institute for Petroleum Research and Geophysics, Holon, Israel
[b] Siberian Research Institute of Geology, Geophysics and Mineral Resources, Novosibirsk, Russia
[c] Atlas Wireline Services, Western Atlas International Inc., Houston, Texas, USA

Accepted 25 January 1996

Abstract

The solution for the half-space model is represented directly in the time domain as computationally stable convolution integrals. The influence of the geoelectric parameters of the earth and transmitter current waveform are then investigated for both infinitesimal and finite-dimensional transmitter loops. Simple empirical formulae are derived to account for the finite duration of the transmitter current turn off time.

The whole transient process is divided into three essentially different stages: the propagation stage, the intermediate stage and the diffusion stage. The first is characterized by extremely complicated signal behavior. Apparently, interpretation of the field data using any kind of model fitting inversion algorithm is impossible in this stage. The diffusion stage virtually coincides with that used in the quasi-static case and is, therefore, unsuitable for detecting the dielectric properties of the earth. The intermediate stage is, thus, the only possible time range in which the dielectric properties can be detected using the dynamic characteristics of the signal.

The duration of each stage is evaluated depending on the geoelectric parameters of the earth for different transmitter current waveforms.

1. Introduction

Unlike the quasi-static case, the behavior of the electromagnetic field in both frequency and time domains with due regard for displacement currents, has been investigated only sporadically in geophysics. The most extensive research in both domains was carried out by Wait and his co-workers (Wait, 1951, 1954, 1962, 1981, 1982; Fuller and Wait, 1972, 1976; Mahmoud et al., 1979). The influence of displacement currents in the frequency domain has been investigated more thoroughly than that in the time domain. The practical reason for such discrimination is quite clear: the frequency range in which the displacement currents may play a significant role (roughly greater than a few MHz) belongs to the working range of several existing geophysical methods. For example, this range has been used for some time in very high frequency borehole dielectric measurements (Poley et al., 1978) as well as in the recently developed shallow surface method for environmental studies known as the short wave electromagnetic sounding method (Stewart, 1990).

PII S0926-9851(96)00006-7

As far as transient electromagnetics is concerned, the time range in which the displacement currents have appreciable influence is so short (approximately less than a few hundred ns) that, until very recently, it was completely outside the measurement range of any existing equipment.

Another, probably no less important, reason for this discrimination is the exceptional complexity of the time domain solutions including displacement currents compared to those in the frequency domain. Unlike the quasi-static case, numerical Fourier (Laplace) transform of the frequency response into the time domain proved to be computationally inefficient within the most interesting time ranges around the arrival times of both direct and reflected (refracted) waves. It is, therefore, no wonder that the abundance of publications concerning frequency domain forward, and even inverse, solutions (Wait, 1954, 1981, 1982; Fuller and Wait, 1972; Sinha, 1977; Alumbaugh and Newman, 1994; Anderson, 1991, 1994a; Lee et al., 1994) has not been accompanied by appropriate investigations of the transient response, including displacement currents. To the best of our knowledge, until very recently only full and half-space models were considered in the time domain (apart from Mahmoud et al., 1979 who dealt with two-layered models in which the displacement currents in the earth were neglected while those in the air were accounted for). In addition to the above publications by Wait and his co-workers, only a few more geophysical contributions refer to this specific subject, all of them dealing with the half-space model only (Bhattacharyya, 1959; Lee, 1981; Weir, 1985).

Although this list does not pretend to be complete, it probably contains all the major geophysical contributions in the field under consideration (transient EM including displacement currents) up until 1993 when the so-called very early transient electromagnetic (VETEM) project was initiated. Since then the VETEM (sometimes called FTEM, fast transient electromagnetic, method) has been developed extensively in various different directions, including instrument design (Wright et al., 1994) system analysis (Labson and Pellerin, 1994) and forward modeling and analysis (Anderson, 1994b; Morrison and Lee, 1994; Tripp et al., 1994). (Note that these works have been published as reports within the framework of the VETEM project and are available only upon request either directly from the authors or from the VETEM project principal investigator, Dr. Louise Pellerin, U.S. Geological Survey, Box 25046, M.S.964, Denver Federal Center, Denver, Colorado 80225, USA; fax: +303-236-1425, e-mail: pellerin@musette.cr.usgs.gov).

2. Time domain solution including displacement currents

Although one would expect the frequency (time dependence) of the earth's electrical properties to have a significant influence in the time range under consideration (Olhoeft, 1994), we shall restrict ourselves by considering the simplest (and in a sense unrealistic) case where electric resistivity (ρ), dielectric permittivity (ϵ) and magnetic permeability (μ) are frequency (time) independent. Given the extremely complicated behavior of the transient electromagnetic field within the propagation time range, it seems methodologically reasonable to examine first a simplified geoelectric model, leaving more practical aspects of the problem to future investigations.

The appropriate frequency-domain solution for the model shown in Fig. 1 is well known (Wait, 1962):

$$A_z = -\frac{M_z i\omega\mu_0}{2\pi}\int_0^\infty \frac{\lambda}{n_0+n_1} J_0(\lambda r)\,\mathrm{d}\lambda \tag{1}$$

where

$$n_j = \sqrt{\lambda^2 + k_j^2}\,;\; k_j^2 = -\omega^2\epsilon_j\mu_0 - i\omega\mu_0\sigma_j;\; \mu_0 = 4\pi\times 10^{-7} H/m,\; j = 0,1$$

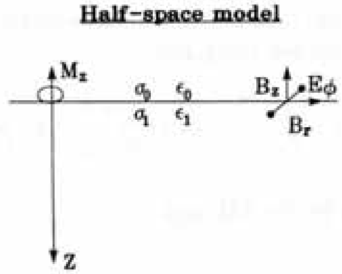

Fig. 1. Model geometry.

and

$$E_\varphi = -\frac{\partial A_z}{\partial r};\ \frac{\partial B_z}{\partial t} = \frac{1}{r}\frac{\partial}{\partial r}\left(r\frac{\partial A_z}{\partial r}\right);\ \frac{\partial B_r}{\partial t} = -\frac{\partial^2 A_z}{\partial r \partial z} \tag{1a}$$

It should be noted that contrary to Wait (1962), we use time dependence $\exp(-i\omega t)$ throughout this paper.

The integral in Eq. (1) can be represented as follows:

$$\int_0^\infty \frac{\lambda}{n_0+n_1} J_0(\lambda r)\mathrm{d}\lambda = \frac{1}{k_0^2-k_1^2}\left(\int_0^\infty \lambda n_0 J_0(\lambda r)\mathrm{d}\lambda - \int_0^\infty \lambda n_1 J_0(\lambda r)\mathrm{d}\lambda\right)$$
$$= \frac{1}{k_0^2-k_1^2}\left(\frac{\partial^2 S_0^*}{\partial z^2}(z=0) - \frac{\partial^2 S_1^*}{\partial z^2}(z=0)\right) \tag{2}$$

where S_j^* is the well known Sommerfeld integral:

$$S_j^* = \int_0^\infty \frac{\lambda}{n_j} e^{-n_j|z|} J_0(\lambda r)\mathrm{d}\lambda = \frac{e^{-k_j R}}{R} \text{ and } R = \sqrt{r^2+z^2} \tag{2a}$$

The Fourier transform of the Sommerfeld integral is well known

$$S_j(t) = \frac{1}{2\pi}\int_{-\infty}^{\infty} \frac{e^{-k_j R}}{R} e^{-i\omega t}\mathrm{d}\omega = -\frac{e^{-\gamma_j t}}{R}\left(I_1(v_j)\frac{\gamma_j^2 T_j}{v_j}u(t-T_j) - I_0(v_j)\delta(t-T_j)\right) \tag{3}$$

where $\gamma_j = 1/2\ \sigma_j/\epsilon_j$; T_j is the arrival time in the jth medium ($T_j = R\cdot\sqrt{\mu_0\epsilon_j}$); I_0 and I_1 are modified Bessel functions of zero and first orders, respectively; $v_j = \gamma_j\sqrt{\tau^2 - T_j^2}$, $u(x)$ is the Heaviside function and $\delta(x)$ is the Dirac delta function.

Unfortunately, the Fourier transform of Eq. (2) cannot be analytically evaluated due to the presence of factor $1/(k_0^2-k_1^2)$. On the other hand, experience shows that the numerical Fourier transform of Eq. (2) is extremely unstable. In order to solve this problem, we suggest applying the well known convolution theorem:

if $G(t) = \frac{1}{2\pi}\int_{-\infty}^{\infty} G^*(\omega)e^{-i\omega t}\mathrm{d}\omega$ and $Q(t) = \frac{1}{2\pi}\int_{-\infty}^{\infty} Q^*(\omega)e^{-i\omega t}\mathrm{d}\omega$ then

$$H(t) = \frac{1}{2\pi}\int_{-\infty}^{\infty} G^*(\omega)Q^*(\omega)e^{-i\omega t}\mathrm{d}\omega = \int_{-\infty}^{\infty} G(t-\tau)Q(\tau)\mathrm{d}\tau \tag{4}$$

Inasmuch as Fourier transforms of all multipliers in Eq. (2) can be analytically evaluated, instead of the numerical Fourier (Laplace) transform, the time domain solution to Eq. (2) can be represented in the form of much more computationally stable convolution integrals:

$$\frac{1}{2\pi}\int_{-\infty}^{\infty} f^*(\omega)\frac{\partial^2}{\partial z^2}\bigg|_{z=0} S_j^*(\omega)e^{-i\omega t}d\omega = \int_{-\infty}^{\infty} f(t-\tau)\frac{\partial^2}{\partial z^2}\bigg|_{z=0} S_j(\tau)d\tau \tag{5a}$$

where $f^*(\omega) = \dfrac{1}{k_0^2 - k_1^2}$. $S_j(t)$ is given by Eq. (3), and:

$$f(x) = \frac{1}{2\pi}\int_{-\infty}^{\infty} \frac{e^{-i\omega x}}{k_0^2 - k_1^2}d\omega \tag{5b}$$

The integral in Eq. (5b), after some trivial transformations, is represented in the form of a tabulated Laplace transform (Abramovitz and Stegun, 1969):

$$f(x) = \frac{1}{\epsilon\mu_0}e^{-\gamma x}\cdot\frac{1}{2\pi i}\int_{\gamma-i\infty}^{\gamma+i\infty}\frac{1}{p^2-\gamma^2}e^{px}dp = \frac{1}{\mu_0\sigma}(1-e^{-2\gamma x})u(x) \tag{5c}$$

where $\sigma = \sigma_1 - \sigma_0$, $\gamma = 1/2\cdot\sigma/\epsilon$ and $\epsilon = \epsilon_1 - \epsilon_0$.

Substituting Eqs. (2) and (2a) into Eqs. (5), (5a) and (5b) and taking into account Eq. (1), we obtain the following equation for the vector-potential in the time domain for the step-function excitation:

$$A_z(t) = \frac{M_z\mu_0}{2\pi}\int_{-\infty}^{\infty} f(t-\tau)\frac{\partial^2}{\partial z^2}\left[S_1(\tau, z=0) - S_0(\tau, z=0)\right]d\tau \tag{6}$$

where $S_j(\tau, z=0)$ and $f(t-\tau)$ are given by Eqs. (3) and (5c), respectively, with $z=0$ and $t-\tau=x$.

In order to obtain the appropriate expressions for the transient EM field components, we must differentiate the right hand side of Eq. (3) along r and z variable three or four times in accordance with Eq. (1a). Omitting intermediate, fairly tiresome calculations, the final expression for the azimuthal electric field component can be represented as follows:

$$E_\varphi(t) = \frac{M_z\mu_0}{2\pi}(A_1 - A_0) \tag{7}$$

where

$$A_j = \frac{T_j^5\gamma_j^4}{\mu_0\sigma r^4}\left\{\left(\int_{-\infty}^{\infty}\varphi_j(\tau)\frac{I_2(v_j)}{v_j^2}u(\tau-T_j)u(t-\tau)d\tau + \varphi_j(T_j)\left(1+\frac{T_j^2\gamma_j^2}{2}\right)u(t-T_j)\right.\right.$$
$$\left.\left. + \varphi_j(T_j)T_j\delta(t-T_j) - \varphi_j'(T_j)\cdot T_j\cdot u(t-T_j)\right)\right\} \tag{7a}$$

$$\varphi_j(x) = -\frac{e^{-\gamma_j x}}{x^2}\left(1+\gamma_j x + e^{-2\gamma(t-x)}(2\gamma x - 1 - \gamma_j x)\right) \tag{7b}$$

$$\varphi_j'(x) = \frac{e^{-\gamma_j x}}{x^3}\left\{2 + 2\gamma_j x + \gamma_j^2 x^2 - e^{-2\gamma(t-x)}\left[(\gamma_j - 2\gamma)^2 x^2 - 4\gamma x + 2\gamma_j x + 2\right]\right\} \tag{7c}$$

$$\gamma_j = \frac{1}{2}\frac{\sigma_j}{\epsilon_j}, T_j = r\sqrt{\mu_0\epsilon_j}; \gamma = \frac{1}{2}\frac{\sigma}{\epsilon}; \sigma = \sigma_1 - \sigma_0; \epsilon = \epsilon_1 - \epsilon_0$$

$v_j = \gamma_j\sqrt{\tau^2 - T_j^2}$; $I_2(x)$ is the modified Bessel function of second order $j = 0,1$.

It should be noted that the following well known property of the Dirac delta-function was widely used in the derivation of Eqs. (7), (7a), (7b) and (7c):

$$\int_a^b f(x')\delta^{(n)}(x'-x)\,\mathrm{d}x' = \begin{cases} 0, & x<a \text{ or } x>b \\ 0.5(-1)^n f^{(n)}(x+0), & x=a \\ 0.5(-1)^n f^{(n)}(x-0), & x=b \\ 0.5(-1)^n\left[f^{(n)}(x-0)+f^{(n)}(x+0)\right], & a<x<b \end{cases} \tag{8}$$

Here, and throughout the paper, the superscript (n) denotes the nth derivative of the appropriate function. The expression for the time derivatives of the magnetic field (Eq. 1a) can be similarly obtained.

If the dielectric permittivity of the earth is equal to that of the air, the expression for the field is significantly simplified. This is due to the fact that multiplier $1/(k_0^2-k_1^2)$ in Eq. (2) equals $1/(i\omega\mu\sigma_1)$ and Eq. (6) does not, therefore, contain the convolution integral. Thus, the expression for the azimuthal electric field for $\epsilon_r=\epsilon_1/\epsilon_0=1$ is represented by:

$$E_\varphi(t)=\frac{M_z\rho_1}{2\pi r^4}T_1^5\gamma_1^2\int_t^\infty e^{-\gamma_1\tau}\frac{v_1 I_1(v_1)-4I_2(v_1)}{(\tau^2-T_1^2)^2}\mathrm{d}\tau \tag{9}$$

This simple equation has been used to test our general solution represented by Eq. (7).

3. Transient response of a dipole (step-function excitation)

The results of calculations of Eqs. (7) and (9) are shown in Figs. 2 and 3. The whole transient process can be divided into three stages according to time elapsed after the transmitter current is switched off at $t=0$:

1. $t<T_0$
2. $T_0<t<T_1$
3. $t>T_1$

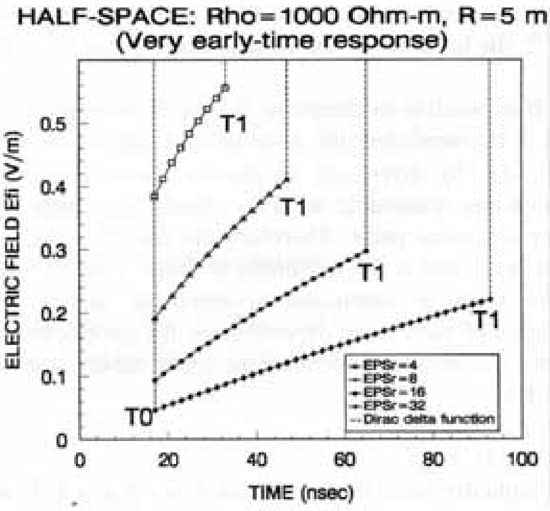

Fig. 2. Transient responses of a dipole (step function excitation) in the propagation stage. Representation of the Dirac delta functions is purely symbolic and serves to designate their position on the time axis only. T_x moment = 1 a·m^2.

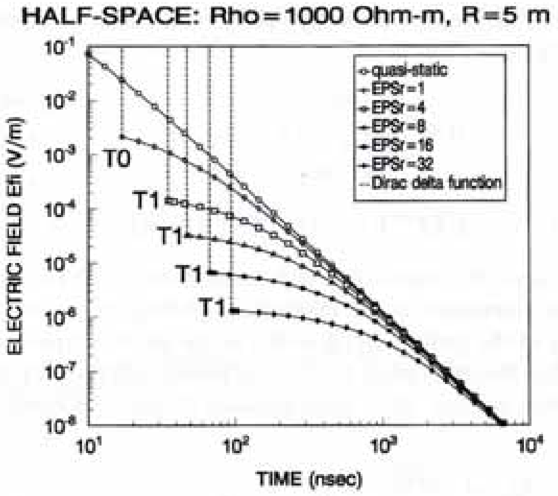

Fig. 3. Transient responses of a dipole (step function excitation) in the intermediate and diffusion stages. Representation of the Dirac delta functions is purely symbolic and serves to designate their position on the time axis only. T_x moment = 1 a·m².

where T_0 and T_1 are the first arrival times through the air and earth respectively ($T_j = r\sqrt{\mu_0 \epsilon_j}$). It is clear that the transient process does not exist in Stage 1 ($E_\varphi = 0$). In Stage 2 the field monotonously increases with time and then drastically decreases (by several orders of magnitude) just after the time $t = T_1 + 0$ (at the beginning of Stage 3). During Stage 3 the signal decays gradually approaching its quasi-static behavior (Fig. 3). It should be noted that such a drastic drop in the signal at time $t = T_1 + 0$ does not allow us to represent all three stages on one figure and the latter is, therefore, separated into two (Figs. 2 and 3).

Precisely at times $t = T_0$ and $t = T_1$, the field is represented by the Dirac delta-function. We shall demonstrate below that this feature disappears if the duration of the turn-off time is non-zero.

The dependence of the signal on the dielectric permittivity of the earth is rather simple if the latter is approximately more than twice as great as that of the free space. The signal is then inversely proportional to the relative dielectric permittivity of the earth during Stage 2 and at the beginning of Stage 3.

However, if ϵ_r is less than 2, the behavior of the field at Stage 2 can be rather complicated, including sign reversals (Table 1).

Thus, theoretically at least, it is possible to determine the dielectric permittivity of the earth during Stage 2 and at the beginning of Stage 3 by measuring the amplitude of the signal in a way similar to that used in traditional geoelectric methods (e.g. by inversion). In practice, however, it is hard to expect that transient response could be measured with any reasonable accuracy shortly after huge spikes which are caused by the arrival of the signal at the measurement point. Therefore the use of signal amplitudes to detect dielectric properties of the earth during Stage 2 and at the beginning of Stage 3 seems unlikely.

Nevertheless, in many cases (such as instrument development, survey design, etc.) it is important to quantitatively evaluate the duration of each stage depending on the geoelectric properties of the earth. From a practical point of view, it is more reasonable to rearrange the above subdivision of the transient process slightly:

1. Propagation stage ($T_0 < t < T_1$)
2. Intermediate stage ($T_1 < t < T_d$)
3. Diffusion (or quasi-static) stage ($t > T_d$)

Here T_0 and T_1 are calculated explicitly using the expression $T_j = r\sqrt{(\mu_0 \epsilon_j)}$. T_d is the time starting from which the measured signal differs by less than 5% from the quasi-static response. T_d can be evaluated either analytically (very roughly) or empirically. The former estimation can be carried out using a well known

Table 1
Half space model with small dielectric contrasts. Transient responses (V/m) of a dipole due to the step-function excitation in the propagation stage

t_{ns}	ϵ_r					
	1	1.2	1.4	1.6	1.8	2.0
16.000	0.000	0.000	0.000	0.000	0.000	0.000
17.000	$0.214E-02$	$-0.127E+02$	$-0.18052E+01$	$0.600E-01$	$0.404E+00$	$0.544E+00$
18.000	$0.214E-02$	$-0.127E+02$	$-0.18052E+01$	$-0.600E-01$	$0.404E+00$	$0.544E+00$
19.000	$0.198E-02$	$0.153E-02$	$-0.69667E+00$	$0.198E+00$	$0.492E+00$	$0.588E+00$
20.000	$0.191E-02$	$0.148E-02$	$0.11712W-02$	$0.295E+00$	$0.528E+00$	$0.607E+00$
21.000	$0.183E-02$	$0.143E-02$	$0.11367E-02$	$0.376E+00$	$0.559E+00$	$0.624E+00$
22.000	$0.177E-02$	$0.138E-02$	$0.11034E-02$	$0.897E-03$	$0.586E+00$	$0.639E+00$
23.000	$0.170E-02$	$0.134E-02$	$0.10714E-02$	$0.873E-03$	$0.723E-03$	$0.652E+00$
24.000	$0.164E-02$	$0.129E-02$	$0.10404E-02$	$0.851E-02$	$0.706E-03$	$0.593E-03$
25.000	$0.158E-02$	$0.125E-02$	$0.10106E-02$	$0.828E-02$	$0.689E-03$	$0.580E-03$
T_1	16.68	18.27	19.73	21.10	22.38	23.59

T_x moment = 1 a · m^2.
Rho = 1000 Ohm-m.
$R = 5$ m.
$T_0 = 16.68$ ns.

quasi-static condition in the frequency domain: $\omega\mu_0\sigma_1 > \omega^2\epsilon_1\mu_0$; then $f < \sigma_1/(2\pi\epsilon_1)$ or, in the time domain, $t > 2\pi\epsilon_1\rho_1 = T_d$. However, calculations show that although the latter expression reflects the general dependence of T_d on both geoelectric parameters, it may lead to significant errors in quantitative evaluation of the duration of the intermediate range and the beginning of the diffusion range. The following empirical formula provides a much better quantitative estimate of T_d:

$$T_d = \rho_1^{0.94}(\epsilon_r + 1) - 21\epsilon_r - 19 \tag{10}$$

where ρ_1 and T_d are calculated in Ohm-m and ns, respectively.

Neither formula shows any dependence on r, but it is clear that the formulae make sense only if $T_d > T_1$. The latter inequality, thus, defines constraints on the transmitter/receiver separation which must be taken into account when applying Eq. (10).

It should be noted that apparently the proposed classification is also valid for more complicated geoelectric models. However, in a general case, Eq. (10) cannot be applied directly and should be used for qualitative estimations only.

4. Transient response of a dipole (exponential excitation)

Contrary to the quasi-static case, the general solution for the step-function excitation includes discontinuous terms (Eq. 7a). Fortunately, these terms disappear if the current waveform is represented by any differentiable function of time. Indeed, the response for an arbitrary excitation is expressed through the step-function response using the well known convolution integral:

$$f^{\text{arb}}(t) = \int_0^t \frac{\varphi^{\text{arb}}}{\partial\tau}(\tau) f^{\text{step}}(t-\tau)\,\mathrm{d}\tau \tag{11}$$

where φ^{arb} is the transmitter current excitation function.

Substituting Eq. (7a) into Eq. (11) and taking into account Eq. (8), it may be seen that the response to an arbitrary excitation $f^{arb}(t)$ no longer includes delta-functions. If, in addition, the first derivative of the excitation function is also a continuous function of time, then the response is also a continuous function; otherwise the response may consist of bounded discontinuities.

Let us consider in some detail the following two exponential turn off time excitations:

$$\begin{aligned} &\varphi_1^{arb}(t) = 1\ (t<0) \quad \text{and} \quad \phi_2^{arb}(t) = 1\ (t<0) \\ &\varphi_1^{arb}(t) = e^{-t/TC}\ (t>0) \quad \text{and} \quad \varphi_2^{arb}(t) = e^{-(t/TC)^2}\ (t>0) \end{aligned} \tag{12}$$

The excitation function $\varphi_1^{arb}(t)$ is presently employed in the pilot version of the USGS VETEM instrument (Wright et al., 1994). It should be noted that, for simplicity's sake, we are considering a single turn off excitation, although the real system employs a series of alternating turn on/turn off excitations.

The time derivative of the excitation function has a discontinuity at $t=0$:

$$\begin{aligned} &(\varphi_1^{arb})' = 0 \qquad (t<0) \\ &(\varphi_1^{arb})' = -\frac{1}{TC}e^{-t/TC} \quad (t>0) \end{aligned} \tag{13}$$

As a result, the response also has bounded discontinuities at $t=T_0$ and $t=T_1$, while delta-functions disappear at these instants.

The response due to the second excitation function, φ_2^{arb}, is a continuous function of t in the whole time range, since the time derivative of φ_2^{arb} is also a continuous function of time:

$$\begin{aligned} &(\varphi_2^{arb})' = 0 \qquad (t<0) \\ &(\varphi_2^{arb})' = -\frac{2t}{TC^2}e^{-(t/TC)^2} \quad (t>0) \end{aligned} \tag{14}$$

Fig. 4 shows responses due to the step-function and both exponential excitations. One can see how the response degenerates from the continuous function of time ($\exp(-t/TC)^2$ – excitation) through bounded discontinuities

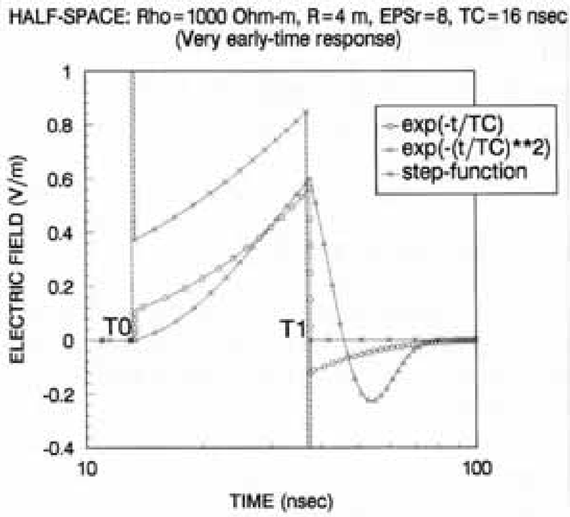

Fig. 4. Transient responses of a dipole due to different excitation functions in the propagation stage. T_x moment = 1 a·m^2.

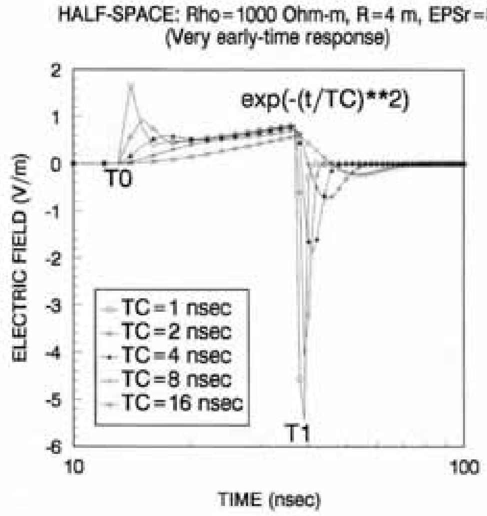

Fig. 5. Transient responses of a dipole due to the exponential excitation with different time constants. T_x moment = 1 a·m^2.

at instants T_0 and T_1 ($\exp(-t/TC)$ – excitation) to the delta-function values at these instants for the step-function excitation.

Fig. 5 shows the responses due to the $\exp(-t/TC)^2$ – excitation for different values of the time constant TC. The response has one positive and one negative maximum at instants T_0 and T_1, respectively. When the time approaches the diffusion (quasi-static) stage, the response changes polarity and then forms an additional positive maximum (not seen on the figure owing to the linear scale used) and finally approaches the quasi-static response.

The first maximum at instant T_0 is available only for sufficiently small time constant values ($TC = 4$ ns in the example under consideration). When the latter decreases indefinitely, both maxima become sharper and finally approach the delta-function value (compare Figs. 4 and 5).

Owing to the linear scale used for the Y-axis in Figs. 4 and 5, it is difficult to identify visually how the exponential responses approach the step-function response at later times. Fig. 6 represents the relatively late time responses for all the above mentioned excitations in the log–log scale. It may be seen that both exponential responses demonstrate similar behavior, but the response for the $\exp(-t/TC)$ – excitation approaches the step-function response at a much later time.

In order to estimate the times at which the exponential responses practically coincide with the step-function response, the calculation for different resistivities, dielectric permittivities, time constants and separations have been carried out resulting in the following empirical formulae:

$$t = 18TC + T_1 \text{ for the } \exp(-t/TC) - \text{excitation} \quad (15)$$

$$t = 5TC + T_1 \text{ for the } \exp(-t/TC)^2 - \text{excitation} \quad (16)$$

5. Transient response of a finite-dimensional transmitter loop

For the sake of convenience, we shall investigate the influence of finite dimensions of the transmitter loop for exponential excitation $\exp(-t/TC)^2$ only.

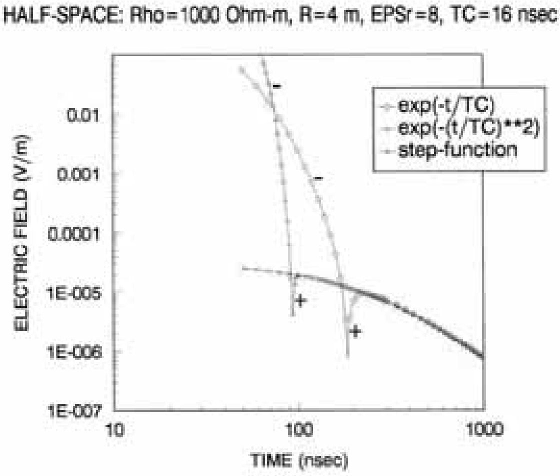

Fig. 6. Transient responses of a dipole due to different excitation functions in the intermediate and diffusion stages. T_x moment = 1 a · m^2.

In order to calculate the response of the loop, the latter is divided into N trapezoidal elements as shown in Fig. 7. Here $N = N_r \text{x} N\varphi$, where N_r is the number of intervals along the r-direction and N_φ is the number of intervals along the φ direction. Note that, owing to symmetry, only half the circle $(0 < \varphi < 180°)$ should be considered. The dipole is placed at the center of the element and the azimuthal component of the electric field, $E_{\varphi'}^{i,j}$ in the appropriate coordinate system, is then calculated using Eqs. (7) and (11). Here $i = 1, \ldots, N_r$ and $j = 1, \ldots, N_\varphi$. The desired azimuthal electric field is first calculated for the elementary dipole:

$$E_{\varphi}^{i,j} = E_{\varphi'}^{i,j} \cos \alpha_{i,j} \tag{17}$$

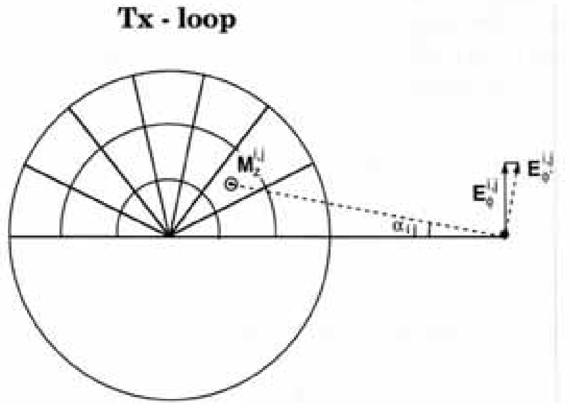

Fig. 7. Geometry used for calculating transient response of a finite dimensional transmitter loop.

Finally,

$$E_\varphi = 2\frac{\sum_{i=1}^{N_r}\sum_{j=1}^{N_\varphi} E_\varphi^{i,j} S_{i,j}}{\sum_{i=1}^{N_r}\sum_{j=1}^{N_\varphi} S_{i,j}} \tag{18}$$

where $S_{i,j}$ is the area of the trapezoidal element and the expression in the denominator describes the area of the semicircle shown in Fig. 7.

It is extremely important to emphasize that, unlike the quasi-static case, the above mentioned algorithm only approximately describes the response of a finite-dimensional loop even if N_r and $N_\varphi \to \infty$. This is because the algorithm does not take into account the final velocity of the signal propagation within the loop which could have a significant influence on the response, at least during the propagation stage. Accounting for all delicate propagation effects within both transmitter and receiver systems should be the subject of a special discussion;

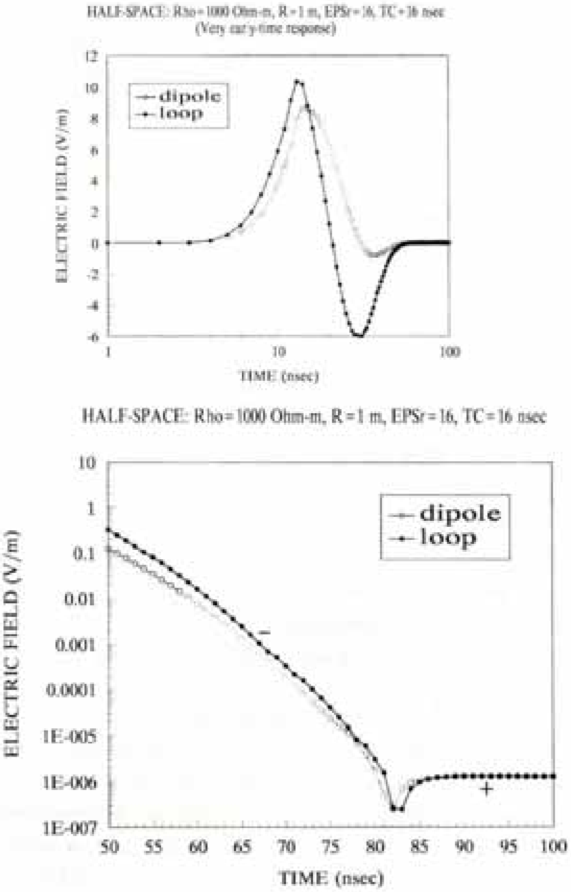

Fig. 8. Transient responses of a dipole and finite transmitter loop for the ratio $R/\alpha = 2$. $R = 1$ m, $\alpha = 0.5$ m, T_x moment $= 1$ a · m^2. (a) Propagation stage. (b) Intermediate and diffusion stages.

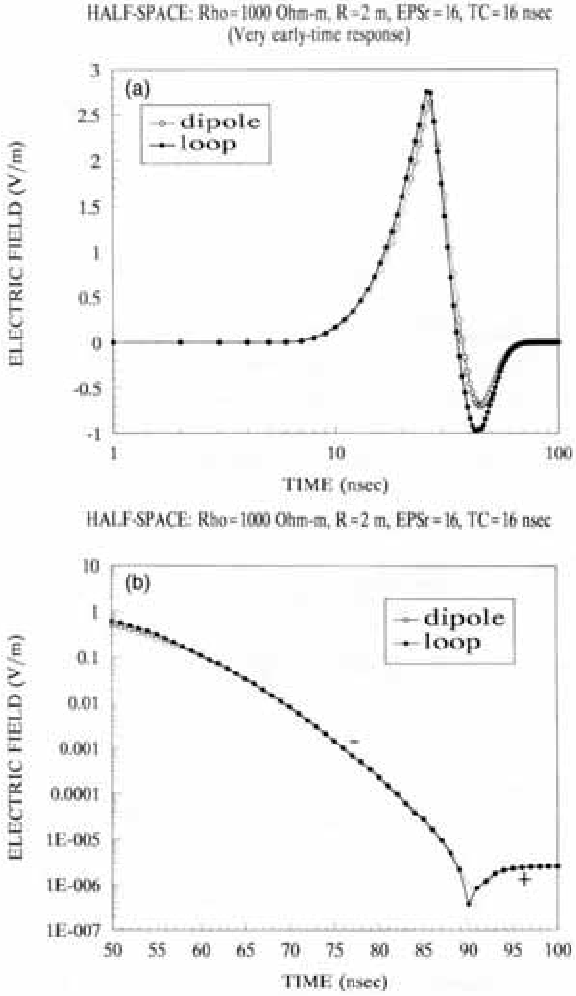

Fig. 9. Transient responses of a dipole and finite transmitter loop for the ratio $R/\alpha = 4$. $R = 2$ m, $\alpha = 0.5$ m, T_x moment = 1 a · m². (a) Propagation stage. (b) Intermediate and diffusion stages.

we shall restrict ourselves here by accounting only for the propagation effects within the earth as if the signal within the transmitter system propagates at infinite speed.

The number of intervals in both directions is chosen empirically by the doubling method, according to which sufficient accuracy is achieved with $N_r = N_\varphi = 5$ for the considered range of geoelectric parameter changes. Fig. 8a,b, Fig. 9a,b, and Fig. 10a,b show the response due to both infinitesimal (vertical magnetic dipole) and finite-dimensional transmitter loops. Similar to the well known quasi-static behavior, the responses approach each other increasing the R/α ratio, where R is the T/R separation and α is the radius of the transmitter loop. However, unlike the quasi-static case, the response may have fairly sharp spikes during the propagation stage and also changes polarity during the intermediate stage. The influence of the finite dimensions of the transmitter loop in the vicinity of these peculiarities is much greater than that in the diffusion stage. Strictly speaking, the responses of the dipole and finite-dimensional loop never completely coincide at these points, no matter how large the ratio R/α (see Figs. 8–10).

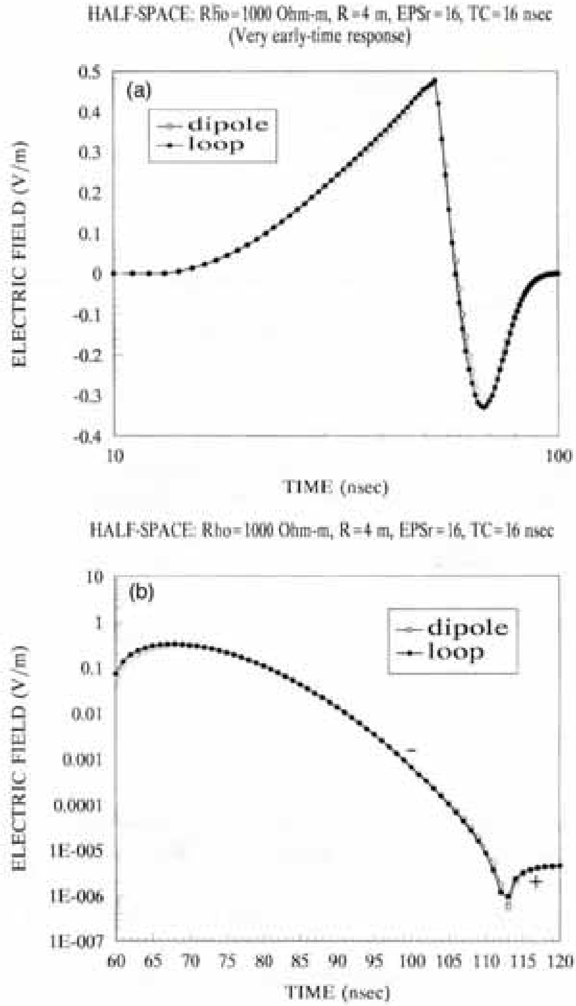

Fig. 10. Transient responses of a dipole and finite transmitter loop for the ratio $R/\alpha = 8$. $R = 4$ m, $\alpha = 0.5$ m, T_x moment $= 1$ a · m². (a) Propagation stage. (b) Intermediate and diffusion stages.

From a practical viewpoint, however, the following inequalities are sufficiently accurate to describe the limits of applicability of the dipole approximation in each of the above mentioned stages separately:

1. Propagation stage: $R/\alpha > 8$
2. Intermediate stage: $R/\alpha > 8$
3. Diffusion stage: $R/\alpha > 1$

It is interesting to note that similar estimations which have been carried out for the early stage response in the quasi-static case (Kaufman and Keller, 1983) showed a much greater ratio of R/α ($R/\alpha > 5$) than we obtained for the diffusion stage. This apparent discrepancy between our results and those of Kaufman and Keller is explained by the fact that, for the above parameters, the intermediate and even propagation stages turn out to be very late stages in the quasi-static case. It is a well known fact that the influence of finite dimensions of the transmitter loop is negligible at this stage.

6. Conclusions

An efficient algorithm for calculating transient response within homogeneous half-space including displacement currents has been developed. The algorithm is based on calculation of numerically stable convolution integrals directly in the time domain.

Numerous calculations have been carried out for the particular case of the azimuthal electric field about an infinitesimal and finite-dimensional transmitter loop located at the earth's surface. We have shown that the transient response for the step-function excitation has a physically meaningless behavior (delta-functions at the first arrival times through air and earth). This behavior disappears as the transmitter current is switched off during finite time. If the excitation function is continuous but its first derivative has discontinuity, the response is a bounded function with finite discontinuities at the arrival times. If the excitation function has a continuous first derivative then the response is also a continuous function of time.

The shape of the response during the propagation and intermediate stages depends heavily on the turn off time duration. The smaller the duration, the sharper the spikes of the response during both arrival times. Under such conditions, any model fitting inversion is hardly possible during the propagation stage or at the start of the intermediate stage. The only time range during which the response is smooth and still depends on dielectric properties of the earth is the second half of the intermediate stage.

The duration of each stage depending on geoelectric properties of the earth and transmitter/receiver separation can be easily estimated using the proposed empirical formulae. Similar formulae are also obtained to estimate the applicability of limits for some important idealized approximations such as dipole source and step-function excitation.

Acknowledgements

This research has been partially supported by the U.S. Geological Survey in the framework of the VETEM project sponsored by the Office of Environment Restoration and Waste Management of the U.S. Department of Energy.

The Israel Ministry of Energy and Infrastructure, through its Earth Sciences Research Administration, has also sponsored our research.

Our thanks are due to Boris Rabinovich for helpful discussions and to Debbie Artzi for typing the manuscript and improving its style.

References

Abramovitz, M. and Stegun, I.A., 1969. Handbook of Mathematical Functions. Dover Publ.

Alumbaugh, D.L. and Newman, G.A., 1994. 3D EM finite-difference modeling on massively parallel computers. VETEM Report.

Anderson, W.L., 1991. Approximate inversion of high frequency electromagnetic soundings using complex image theory. Geophysics, 56: 1087–1092.

Anderson, W.L., 1994a. Q-factor approximation of electromagnetic fields for high frequency sounding in the 300 kHz to 30 MHz range over layered media. USGS Report.

Anderson, W.L., 1994b. VETEM-2. VETEM Report.

Bhattacharyya, B.K., 1959. Electromagnetic fields of a transient magnetic dipole on the earth's surface. Geophysics, 25: 89–108.

Fuller, J.A. and Wait, J.R., 1972. High frequency EM coupling between small coplanar loops over an inhomogeneous ground. Geophysics, 37: 997–1004.

Fuller, J.A. and Wait, J.R., 1976. A pulsed dipole in the earth. In: L.B. Folser (Editor), Topics in Applied Physics: Transient Electromagnetic Fields, 10: 237–269.

Kaufman, A.A. and Keller, G.V., 1983. Frequency and Transient Soundings. Elsevier, Amsterdam.

Labson, V. and Pellerin, L., 1994. Untitled VETEM report.

Lee, K.H., Xie, G. and Morrison, F., 1994. 3D high frequency EM modeling. VETEM Report.

Lee, T., 1981. The effect of displacement currents on the time domain EM fields. Bull. Aust. Soc. Explor. Geophysics, 12: 34–36.

Mahmoud, S.F., Botros, A.Z. and Wait, J.R., 1979. Transient electromagnetic fields of a verticaL magnetic dipole on a two-layer earth. Proceedings of the IEEE, vol. 67, pp. 1022–1029.

Morrison, H.F. and Lee, K.H., 1994. Early time response of a layered half space. VETEM Report.

Olhoeft, H., 1994. Laboratory measurements of the electrical and magnetic properties over the frequency range from 1 to 1,000 MHz. VETEM Report.

Poley, J.Ph., Nooteboom, J.J. and de Waal, P.J., 1978. Use of VHF dielectric measurements for borehole formation analysis. Log Analyst, pp. 8–30.

Sinha, A.K., 1977. Influence of altitude and displacement currents on plane-wave EM fields. Geophysics, 42: 77–91.

Stewart, D.C., 1990. Detection of shallow subsurface layers by high frequency electromagnetic sounding. Ph.D. Thesis, Colorado School of Mines.

Tripp, A., Wang, T. and Xiong, Z., 1994. Untitled VETEM Report.

Wait, J.R., 1951. Transient electromagnetic propagation in a conducting medium. Geophysics, 16: 213–221.

Wait, J.R., 1954. Mutual couplings of loops lying on the ground. Geophysics, 13: 290–296.

Wait, J.R., 1962. Electromagnetic Waves in Stratified Media. MacMillan.

Wait, J.R., 1981. Wave Propagation Theory. Pergamon Press.

Wait, J.R., 1982. Geoelectromagnetism. Academic Press.

Weir, G.J., 1985. Forerunners on conducting surfaces: the infinitesimal vertical magnetic dipole with displacement terms. Geophys. J. R. Astr. Soc., 81: 19–31.

Wright, D., Grover, T. and Bradley, J., 1994. Status of the time domain system instrumentation. VETEM Report.